HiLL PUBLISHING

**Journal of Applied Mathematics and Computation, 2022, 6(3), 356-369**
https://www.hillpublisher.com/journals/JAMC/
ISSN Online: 2576-0653
ISSN Print: 2576-0645

# Analysis of Bifurcation and Chaos to Fractional Order Brusselator Model

**Md. Jasim Uddin**

Department of Mathematics, University of Dhaka, Dhaka, Bangladesh.

**How to cite this paper:** Md. Jasim Uddin. (2022) Analysis of Bifurcation and Chaos to Fractional Order Brusselator Model. *Journal of Applied Mathematics and Computation*, 6(3), 356-369.
DOI: 10.26855/jamc.2022.09.008

**Received:** July 22, 2022
**Accepted:** August 18, 2022
**Published:** September 21, 2022

***Corresponding author:** Md. Jasim Uddin, Department of Mathematics, University of Dhaka, Dhaka, Bangladesh.
**Email:** jasim.uddin@du.ac.bd

## Abstract

The Caputo fractional derivative has been considered the Brusselator model. A discretization procedure is initially used to construct caputo fractional differential equations for Brusselator model. We list the topological categories for this model fixed points. Then, we demonstrate analytically that a fractional order Brusselator model underpins a Neimark-Sacker (NS) bifurcation and a Flip-bifurcation under specific parametric conditions. We establish the existence and direction of NS and Flip bifurcations by employing central manifold and bifurcation theory. The dynamical behavior of the fractional order Brusselator model has been determined to be extremely sensitive to the parameter values and the initial conditions. It is investigated how the model's dynamics are affected by step size and fractional- order parameters. We run numerical simulations to support our analytic results, including bifurcations, phase portraits, periodic orbits, invariant closed cycles, rapid emergence of chaos, and abrupt removal of chaos. Finally, a hybrid control method is used to stop the systems chaotic trajectory.

## Keywords

Fractional order Brusselator model, Flip and Neimark-Sacker (NS) Bifurcations, Phase portraits, Chaos control

## 1. Introduction

The study of the various ways to define real number powers or complex number powers of the differentiation operator is done through the discipline of mathematical analysis known as fractional calculus. The concept of fractional calculus dates back to the 17th century. It might be thought of as a fresh research subject, nevertheless. Many mathematically specified epidemiological models have been developed over time [1, 2] but the majority of these models are limited to differential equations of integer order (IDEs). In the last 30 years, fractional-order differential equations have been successfully described in a wide range of fields, including science, engineering, finance, economics, and epidemiology [3-7]. These fractional-order models have a nonlocal characteristic, which is absent from IDEs. Nonlocal property denotes that a model's subsequent state depends on all of its previous states in addition to its current state [8]. When switching from an integer-order model to a fractional-order model, the order of differentiation $\alpha$ must be precise; even a small change in the order of differentiation $\alpha$ could have a big impact on the final result [9]. Some phenomena that IDEs cannot sufficiently model can be modeled using FDEs [10]. FDEs are frequently used to biological systems since these systems naturally relate to memory-based systems. A nonlinear fractional differential system may exhibit complicated dynamics, including chaos and bifurcation, just like a nonlinear differential system does. The topic of studying chaos in fractional-order dynamical systems is appealing and fascinating [11, 16, 17, 18, 19]. Applying the idea of differentiation to arbitrary order can be done in a variety of ways. The definitions proposed by Riemann-Liouville, Caputo, and Grünwald-Letnikov are the most widely used ones [12].

Applied mathematicians are looking into a number of additional tactics in addition to these definitions. In creating or changing their models, researchers are always searching for the most efficient method, including certain numerical methods [13, 14, 15].

The Neimark-Sacker and flip bifurcations, stable orbits, and chaotic attractors are among the many discrete systems that have piqued researchers curiosity [20, 21]. These phenomena can be quantified numerically or using normal form and center manifold theory.

In this paper a fractional order Brusselator model is considered. In addition to the two parameters previously present in the initial Brusselator model suggested in [28], this model also includes a fractional-order parameter and a time step parameter. As these parameters are altered, bifurcations are observed as indicated in sect. 4.In 1968, Prigogine and Lefever [22, 23] published their groundbreaking study on the oscillating chemical reaction known as the Brusselsator reaction. The non-dimensional form of hypothetical Brusselator Model is given below

$$\begin{aligned} \dot{x} &= a - (1+b)x + x^2 y \\ \dot{y} &= bx - x^2 y \end{aligned} \tag{1}$$

where $x$ and $y$ proportional to two chemical reactants and the parameters $a$ and $b$ are two positive constants.

The Brusselator model of fractional order is provided as follows.

$$\begin{aligned} D^{\alpha}x(t) &= a - (1+b)x(t) + x^2(t)y(t) \\ D^{\alpha}y(t) &= bx(t) - x^2(t)y(t) \end{aligned} \tag{2}$$

where $t > 0$, and $\alpha$ is the fractional order which satisfy $\alpha \in (0, 1]$. This type of system can be discretized using a variety of techniques. A representative of them is the piecewise constant approximation. With this approach, the model is discretized. The process is given as follows:

Let the initial conditions of system (1) are $x(0) = x_0, y(0) = y_0$. The following is the discretized form of system (2):

$$\begin{aligned} D^{\alpha}x(t) &= a - (1+b)x\left(\left[\frac{t}{\rho}\right]\rho\right) + x^2\left(\left[\frac{t}{\rho}\right]\rho\right)y\left(\left[\frac{t}{\rho}\right]\rho\right) \\ D^{\alpha}y(t) &= bx\left(\left[\frac{t}{\rho}\right]\rho\right) - x^2([\tfrac{t}{\rho}]\rho)y([\tfrac{t}{\rho}]\rho) \end{aligned} \tag{3}$$

First, let $t \in [0, \rho)$, so $\frac{t}{\rho} \in [0, 1)$. Thus, we obtain

$$\begin{aligned} D^{\alpha}x(t) &= a - (1+b)x_0 + {x_0}^2 y_0 \\ D^{\alpha}y(t) &= bx_0 - {x_0}^2 y_0 \end{aligned} \tag{4}$$

The solution of (4) is reduced to

$$\begin{aligned} x_1(t) &= x_0 + J^{\alpha}(a - (1+b)x_0 + {x_0}^2 y_0) = x_0 + \frac{t^{\alpha}}{\alpha\Gamma(\alpha)}(a - (1+b)x_0 + {x_0}^2 y_0) \\ y_1(t) &= y_0 + J^{\alpha}(bx_0 - {x_0}^2 y_0) = y_0 + \frac{t^{\alpha}}{\alpha\Gamma(\alpha)}(bx_0 - {x_0}^2 y_0) \end{aligned} \tag{5}$$

Second, let $t \in [\rho, 2\rho)$, so $\frac{t}{\rho} \in [1, 2)$. Then

$$\begin{aligned} D^{\alpha}x(t) &= a - (1+b)x_1 + {x_1}^2 y_1 \\ D^{\alpha}y(t) &= bx_1 - {x_1}^2 y_1 \end{aligned} \tag{6}$$

which have the following solution

$$\begin{aligned} x_2(t) &= x_1(\rho) + J_{\rho}^{\alpha}\,(a - (1+b)x_1 + {x_1}^2 y_1) \\ &= x_1(\rho) + \frac{(t-\rho)^{\alpha}}{\alpha\Gamma(\alpha)}(a - (1+b)x_1 + {x_1}^2 y_1) \\ y_2(t) &= y_1(\rho) + J_{\rho}^{\alpha}\,(bx_1 - {x_1}^2 y_1) \\ &= y_1(\rho) + \frac{(t-\rho)^{\alpha}}{\alpha\Gamma(\alpha)}(bx_1 - {x_1}^2 y_1) \end{aligned} \tag{7}$$

where $J_{\rho}^{\alpha} = \frac{1}{\Gamma(\alpha)}\int_{\rho}^{t}(t-\tau)^{\alpha-1}d\tau, \alpha > 0$.When the discretization procedure is repeated n times, we get

$$x_{n+1}(t) = x_n(n\rho) + \frac{(t-n\rho)^{\alpha}}{\alpha\Gamma(\alpha)}\big(a - (1+b)x_n(n\rho) + {x_n}^2(n\rho)y_n(n\rho)\big),$$

$$y_{n+1}(t) = y_n(n\rho) + \frac{(t-n\rho)^{\alpha}}{\alpha\Gamma(\alpha)}\left(bx_n(n\rho) - {x_n}^2(n\rho)y_n(n\rho)\right), \tag{8}$$

where $t \in [n\rho, (n+1)\rho)$. For $t \to (n+1)\rho$, system (8) reduced to

$$x_{n+1} = x_n + \frac{\rho^{\alpha}}{\alpha\Gamma(\alpha)}(a - (1+b)x_n + {x_n}^2 y_n),$$
$$y_{n+1} = y_n + \frac{\rho^{\alpha}}{\alpha\Gamma(\alpha)}(bx_n - {x_n}^2 y_n), \tag{9}$$

The remaining part of this paper is organized as follows: In Sect. 2, the topological divisions of fixed points are investigated. In Sect. 3, we show analytically that the system (9), under a specific parametric condition, experiences a Flip or NS bifurcation. In Sect. 4, we quantitatively display system dynamics, including bifurcation diagrams and phase portraits, to corroborate our analytical findings. In Sect. 5, we employ a hybrid control approach to reduce the unmanaged system's turbulence. In Sect. 6, we provide a brief discussion.

## 2. Stability Analysis

There is just one fixed point in the system (9) $E(x^*, y^*)$, where $x^* = a$ and $y^* = \frac{b}{a}$ which exist regardless of the parameter values that are allowed.

The Jacobian matrix of system (9) evaluated at $E(x^*, y^*)$ are

$$J(x^*, y^*) = \begin{pmatrix} (1 + (-1 + 2x^*y^* - b)\frac{\rho^{\alpha}}{\Gamma(1+\alpha)}) & {x^*}^2\frac{\rho^{\alpha}}{\Gamma(1+\alpha)} \\ (-2x^*y^* + b)\frac{\rho^{\alpha}}{\Gamma(1+\alpha)} & (1 - {x^*}^2)\frac{\rho^{\alpha}}{\Gamma(1+\alpha)} \end{pmatrix} \tag{10}$$

Now the Jacobian matrix at $E(a, \frac{b}{a})$ is given by

$$J_E = \begin{pmatrix} 1 + (-1+b)\frac{\rho^{\alpha}}{\Gamma(1+\alpha)} & a^2\frac{\rho^{\alpha}}{\Gamma(1+\alpha)} \\ -b\frac{\rho^{\alpha}}{\Gamma(1+\alpha)} & 1 - a^2\frac{\rho^{\alpha}}{\Gamma(1+\alpha)}) \end{pmatrix} \tag{11}$$

We can express the characteristic polynomial of the Jacobian matrix as follows:

$$F(\lambda) := \lambda^2 - Tr(J_E)\lambda + Det(J_E) = 0 \tag{12}$$

where $Tr(J_E)$ is the trace and $Det(J_E)$ is the determinant of the Jacobian matrix $J_E$, and is given by

$$Tr(J_E) = 2 + (-1 - a^2 + b)\frac{\rho^{\alpha}}{\Gamma(1+\alpha)}$$
$$Det(J_E) = 1 + (-1 - a^2 + b)\frac{\rho^{\alpha}}{\Gamma(1+\alpha)} + a^2\left(\frac{\rho^{\alpha}}{\Gamma(1+\alpha)}\right)^2 \tag{13}$$

It is possible to write the eigenvalues of (12) as $\lambda_{1,2} = \frac{Tr(J_E) \pm \sqrt{(Tr(J_E))^2 - 4Det(J_E)}}{2}$.

Jury Criterion: *The prerequisite for the equilibrium point $E(x^*, y^*)$ stability is given as follows* $F(1) > 0, F(-1) > 0, F(0) - 1 < 0$.

Let,

$$PD_E = \left\{(a, b, \rho, \alpha): \rho = \left(\Gamma(1+\alpha).\frac{-\ddot{B}_2 \pm \sqrt{L_1}}{\ddot{B}_1}\right)^{\frac{1}{\alpha}} = \rho_{\pm}, L_1 \geq 0\right\}.$$

where,

$$\ddot{B}_1 = a^2; \ddot{B}_2 = -(1 + a^2 - b); \ddot{B}_3 = 4$$
$$L_1 = {\ddot{B}_2}^2 - \ddot{B}_3 * \ddot{B}_1$$

When the parameters $(a, b, \rho, \alpha)$ change within a tiny region of $PD_E$, the system (9) experiences a flip bifurcation at $E$.

Also let

$$NS_E = \left\{(a, b, \rho, \alpha): \rho = \left(\Gamma(1+\alpha).\frac{-\ddot{B}_2}{\ddot{B}_1}\right)^{\frac{1}{\alpha}} = \rho_{NS}, L_1 < 0\right\}$$

When the parameters $(a, b, \rho, \alpha)$ fluctuate in a limited region around of $NS_E$, the system (9) experiences a NS bifurcation at $E$.

We provide the following Lemma for the fixed point $E$'s stability requirement.

**Lemma 1.** *For any arbitrary choice of parameter values, the fixed point E is a sink if*

$$(i)\ L_1 \geq 0, \rho < \rho_-(stable\ node),$$
$$(ii)\ L_1 < 0, \rho < \rho_{NS}(stable\ focus),$$

*source if*

$$(i)\ L_1 \geq 0, \rho < \rho_+(unstable\ node),$$
$$(ii)\ L_1 < 0, \rho > \rho_{NS}(unstable\ focus),$$

*non-hyperbolic*

$$(i)\ L_1 \geq 0, \rho = \rho_-\ or\ \rho = \rho_+(saddle\ with\ flip),$$
$$(ii)\ L_1 < 0, \rho = \rho_{NS}(\ focus),$$

*saddle: otherwise*

## 3. Bifurcation Analysis

By utilizing center-manifold and bifurcation theory [25, 26, 27], we will explore the presence, direction, and stability analysis of flip and NS bifurcations close to the fixed point $E$ in this section. We consider order of the fractional derivative $\alpha$ as the bifurcation parameter, otherwise stated.

### 3.1 Flip Bifurcation

We randomly select the parameters $(a, b, \rho, \alpha)$ place them in $PD_E$. Take into account system (9) at equilibrium point $E(x^*, y^*)$. Think that the parameters are in $PD_E$.

Let,

$$\rho = \left(\Gamma(1+\alpha).\frac{-\ddot{B}_2 - \sqrt{L_1}}{\ddot{B}_1}\right)^{\frac{1}{\alpha}} = \rho_-, L_1 \geq 0.$$

And the eigenvalues of $J_E$ are given as

$$\lambda_1 = -1 \text{ and } \lambda_2 = 3 + \ddot{B}_2\rho_-$$

In order for $|\lambda_2| \neq 1$ gives $\ddot{B}_2\rho_- \neq -2, -4$ (14)

We then employ the transformation $\hat{x} = x - x^+, \hat{y} = y - y^+$ and set $A(\delta) = J(x^*, y^*)$. The fixed point of system (9) is moved to the origin. Hence, the system (9) can be expressed as

$$\begin{pmatrix}\hat{x}\\ \hat{y}\end{pmatrix} \to A(\rho_-)\begin{pmatrix}\hat{x}\\ \hat{y}\end{pmatrix} + \begin{pmatrix}F_1(\hat{x}, \hat{y}, \rho_-)\\ F_2(\hat{x}, \hat{y}, \rho_-)\end{pmatrix} \tag{15}$$

where $X = (\hat{x}, \hat{y})^T$ and

$$F_1(\hat{x}, \hat{y}, \rho_-) = \frac{1}{\ddot{B}_1}\hat{x}^2\hat{y}\left(-\ddot{B}_2 - \sqrt{L_1}\right) + \frac{1}{2}\left[\frac{1}{a}4\hat{x}\hat{y}\left(-\ddot{B}_2 - \sqrt{L_1}\right) + \frac{1}{a^3}2\hat{x}^2 b\left(-\ddot{B}_2 - \sqrt{L_1}\right)\right]$$
$$F_2(\hat{x}, \hat{y}, \rho_-) = -\frac{1}{\ddot{B}_1}\hat{x}^2\hat{y}\left(-\ddot{B}_2 - \sqrt{L_1}\right) - \frac{1}{2}\left[\frac{1}{a}4\hat{x}\hat{y}\left(-\ddot{B}_2 - \sqrt{L_1}\right) + \frac{1}{a^3}2\hat{x}^2 b\left(-\ddot{B}_2 - \sqrt{L_1}\right)\right] \tag{16}$$

The system (15) can be written as follows:

$$X_{n+1} = AX_n + \frac{1}{2}B(X_n, X_n) + \frac{1}{6}C(X_n, X_n, X_n) + O(\|X_n\|^4)$$

where $B(x, y) = \begin{pmatrix}B_1(x, y)\\ B_2(x, y\end{pmatrix}$ and $C(x, y, v) = \begin{pmatrix}C_1(x, y, v)\\ C_2(x, y, v)\end{pmatrix}$are multi-linear vector functions of $x, y, v \in \mathbb{R}^2$ that are symmetric and defined as follows:

$$B_1(x, y) = \sum_{j,k=1}^{2}\frac{\delta^2 F_1(\varepsilon, \rho)}{\delta\varepsilon_j\delta\varepsilon_k}\bigg|_{\varepsilon=0} x_j y_k = \frac{-2}{a^3}(x_2 y_1 a^2 + x_1 y_1 b + x_1 y_2 a^2)\left(\ddot{B}_2 + \sqrt{L_1}\right)$$

$$B_2(x,y)=\sum_{j,k=1}^{2}\frac{\delta^2F_2(\varepsilon,\rho)}{\delta\varepsilon_j\delta\varepsilon_k}\Bigg|_{\varepsilon=0} x_j y_k=\frac{2}{a^3}(x_2y_1a^2+x_1y_1b+x_1y_2a^2)\left(\ddot{B}_2+\sqrt{L_1}\right)$$

and

$$C_1(x,y,v)=\sum_{j,k,l=1}^{2}\frac{\delta^2F_1(\varepsilon,\rho)}{\delta\varepsilon_j\delta\varepsilon_k\delta\varepsilon_l}\Bigg|_{\varepsilon=0} x_j y_k v_l=\frac{-1}{a^2}2\left(\ddot{B}_2+\sqrt{L_1}\right)(v_2x_1y_1+v_1x_2y_1+v_1x_1y_2)$$

$$C_2(x,y,v)=\sum_{j,k,l=1}^{2}\frac{\delta^2F_1(\varepsilon,\rho)}{\delta\varepsilon_j\delta\varepsilon_k\delta\varepsilon_l}\Bigg|_{\varepsilon=0} x_j y_k v_l=\frac{1}{a^2}2\left(\ddot{B}_2+\sqrt{L_1}\right)(v_2x_1y_1+v_1x_2y_1+v_1x_1y_2)$$

Let, $q_1, q_2 \in \mathbb{R}^2$ be two eigenvectors of A and $A^T$ for eigenvalue $\lambda_1(\rho_-) = -1$ such that

$$A(\rho_-)q_1 = -q_1 \text{ and } A^T(\rho_-)q_2 = -q_2.$$

Using a straightforward computation, we then obtain,

$$q_1=\begin{pmatrix}\frac{(\ddot{B}_1(-1+a^2-b+\sqrt{L_1}))}{b(\ddot{B}_2+\sqrt{L_1})}\\1\end{pmatrix}=\begin{pmatrix}q_{11}\\1\end{pmatrix};$$

$$q_2=\begin{pmatrix}\frac{1-a^2+b+\sqrt{L_1}}{(\ddot{B}_2+\sqrt{L_1})}\\1\end{pmatrix}=\begin{pmatrix}q_{21}\\1\end{pmatrix}$$

In order to get, $< q_1, q_2 >= 1$, where $< q_1, q_2 >= q_{11}q_{21} + q_{12}q_{22}$, use of the normalized vector is required as $q_2 = \gamma_F q_2$, with $\gamma_F = \frac{1}{1+q_{11}q_{21}}$.

We must examine the sign of $l_1(\rho_-)$, the coefficient of critical normal form, to determine the direction of the flip bifurcation [24].

$$l_1(\rho_-) = \frac{1}{6} < q_2, C(q_1,q_1,q_1) > -\frac{1}{2} < q_2, B(q_2,(A-I)^{-1}B(q_1,q_1)) > \tag{17}$$

The direction and stability of the Flip bifurcation may be shown in the following ways, in light of the explanation above theorem.

Theorem 1. *Suppose (14) is true and $l_1(\rho_-) \neq 0$, Flip bifurcation will occur for system (9) at fixed point $E(x^*, y^*)$ if the $\rho$ changes its value in a tiny region around $PD_E$. Additionally, there exists an attractive (resp. repelling) smooth closed invariant curve bifurcate from $E(x^*, y^*)$, and the bifurcation is sub-critical(resp. super-critical) if $l_1(\rho_-) < 0$(resp. $l_1(\rho_-) > 0$).*

### 3.2 Neimark-Sacker Bifurcation

When $L_1 < 0$ and the parameters $(a, b, \rho, \alpha) \in NS_E$, then the eigenvalues of system (12) are provided by

$$\lambda, \bar{\lambda} = \frac{Tr(J_E) \pm \sqrt{4Det(J_E) - Tr(J_E)^2}}{2} \tag{18}$$

Let, $\rho = \rho_{NS} = \left(\Gamma(1+\alpha).\frac{-\ddot{B}_2}{\ddot{B}_1}\right)^{\frac{1}{\alpha}}$

Additionally, the non-resonance and transversality criteria result in

$$\frac{d|\lambda_i(\rho)|}{d\rho}\Bigg|_{\rho=\rho_{NS}} \neq 0$$

$$-(Tr(J_E))|_{\rho=\rho_{NS}} \neq 0 \Rightarrow \frac{\ddot{B}_2^{\,2}}{\ddot{B}_1} \neq 2,3 \tag{19}$$

We then employ the transformation $\hat{x} = x - x^+, \hat{y} = y - y^+$ and set $A(\delta) = J(x^*, y^*)$. The fixed point of system (9) is moved to the origin. Hence, the system (9) can be expressed as

$$X = A(\rho)X + F \tag{20}$$

where $X = (\hat{x}, \hat{y})^T$ and $F = (F_1, F_2)^T$ are given by

$$F_1(\hat{x},\hat{y},\rho_{NS}) = -\frac{\ddot{B}_2}{\ddot{B}_1}\hat{x}^2\hat{y} + \frac{1}{2}\left[\frac{-1}{a^3}2\hat{x}^2 b(\ddot{B}_2) - \frac{1}{a}4\hat{x}\hat{y}(\ddot{B}_2)\right]$$
$$F_2(\hat{x},\hat{y},\rho_{NS}) = \frac{\ddot{B}_2}{\ddot{B}_1}\hat{x}^2\hat{y} + \frac{1}{2}\left[\frac{1}{a^3}2\hat{x}^2 b(\ddot{B}_2) + \frac{1}{a}4\hat{x}\hat{y}(\ddot{B}_2)\right] \quad (21)$$

The system (20) can be written as follows

$$X_{n+1} = AX_n + \frac{1}{2}B(X_n,X_n) + \frac{1}{6}C(X_n,X_n,X_n) + O(\|X_n\|^4)$$

where $B(x,y) = \begin{pmatrix} B_1(x,y) \\ B_2(x,y \end{pmatrix}$ and $C(x,y,v) = \begin{pmatrix} C_1(x,y,v) \\ C_2(x,y,v) \end{pmatrix}$ are multi-linear vector functions of $x,y,v \in \mathbb{R}^2$ that are symmetric and defined as follows:

$$B_1(x,y) = \frac{-2}{a^3}(x_2y_1a^2 + x_1y_1b + x_1y_2a^2)(\ddot{B}_2)$$
$$B_2(x,y) = \frac{2}{a^3}(x_2y_1a^2 + x_1y_1b + x_1y_2a^2)(\ddot{B}_2)$$

and

$$C_1(x,y,v) = \frac{-2\ddot{B}_2}{a^2}(v_2x_1y_1 + v_1x_2y_1 + v_1x_1y_2)$$
$$C_2(x,y,v) = \frac{2\ddot{B}_2}{a^2}(v_2x_1y_1 + v_1x_2y_1 + v_1x_1y_2)$$

Suppose, $q_1, q_2 \in \mathbb{C}^2$ be two eigenvectors of A and $A^T$ for eigenvalue $\lambda(\rho_{NS}), \bar{\lambda}(\rho_{NS})$ such that

$$A(\rho_{NS})q_1 = \lambda(\rho_{NS})q_1, A(\rho_{NS})\overline{q_1} = \bar{\lambda}(\rho_{NS})\overline{q_1}$$

And

$$A^T(\rho_{NS})q_2 = \bar{\lambda}(\rho_{NS})q_2,\ A^T(\rho_{NS})\overline{q_2} = \lambda(\rho_{NS})\overline{q_2} \quad (22)$$

Thus, by way of straight computation, we have

$$q_1 = \begin{pmatrix} \frac{1-a^4-2b+b^2+\ddot{B}_2\sqrt{L_1}}{-2b\ddot{B}_2} \\ 1 \end{pmatrix} = \begin{pmatrix} \eta_1 + i\eta_2 \\ 1 \end{pmatrix};$$
$$q_2 = \begin{pmatrix} \frac{-1+a^4+2b-b^2+\ddot{B}_2\sqrt{L_1}}{-2\ddot{B}_1\ddot{B}_2} \\ 1 \end{pmatrix} = \begin{pmatrix} \vartheta_1 + i\vartheta_2 \\ 1 \end{pmatrix}$$

where $\eta_1 = \frac{1-a^4-2b+b^2}{2b\ddot{B}_2}$; $\eta_2 = \frac{-\sqrt{-L_1}}{2b}$

and $\vartheta_1 = \frac{-1+a^4+2b-b^2}{-2\ddot{B}_1\ddot{B}_2}$; $\vartheta_2 = \frac{-\sqrt{-L_1}}{2\ddot{B}_1}$

For $\underset{1}{<} q_1, q_2 > = 1$, where $< q_1, q_2 > = q_{11}q_{21} + q_{12}q_{22}$, use the normalized vector as $q_2 = \gamma_{Ns}q_2$, with $\gamma_{NS} = \frac{1}{1+(\vartheta_1+i\vartheta_2)(\eta_1-i\eta_2)}$.

So the eigenvectors are computed as follows:

$$q_1 = \begin{pmatrix} \eta_1 + i\eta_2 \\ 1 \end{pmatrix};$$
$$q_2 = \begin{pmatrix} \frac{\vartheta_1 + i\vartheta_2}{1+(\vartheta_1+i\vartheta_2)(\eta_1-i\eta_2)} \\ \frac{1}{1+(\vartheta_1+i\vartheta_2)(\eta_1-i\eta_2)} \end{pmatrix}$$

We decompose $X \in \mathbb{R}^2$ as $X = zq_1 + \bar{z}\bar{q_1}$ by taking into account $\rho$ vary near to $\rho_{NS}$ and for $z \in \mathbb{C}$. The explicit formula of $z$ is $z = \langle q_2, X \rangle$. Consequently, the system (9) changed to the following system for $|\rho|$ close to $\rho_{NS}$:

$$z \to \lambda(\rho)z + \hat{g}(z,\bar{z},\rho) \quad (23)$$

where $\lambda(\rho) = (1+\varphi(\rho))e^{i\theta\rho}$ with $\varphi(\rho_{NS}) = 0$ and $\hat{g}(z,\bar{z},\rho)$ is a smooth complex-valued function.
After Taylor expression of $g$ with respect to $(z,\bar{z})$, we obtain

$$\hat{g}(z,\bar{z},\rho)=\sum_{k+l\geq 2}\frac{1}{k!l!}\widehat{g_{kl}}(\rho)z^k z^{-l},\ \text{with}\ \widehat{g_{kl}}\in\mathbb{C},k,l=0,1,\ldots$$

According to multilinear symmetric vector functions, the coefficients $g_{kl}$ are

$$\widehat{g_{20}}(\rho_{NS})=\langle q_2,B(q_1,q_1)\rangle,\widehat{g_{11}}(\rho_{NS})=\langle q_2,B(q_1,\bar{q_1})\rangle$$
$$\widehat{g_{02}}(\rho_{NS})=\langle q_2,B(\bar{q_1},\bar{q_1})\rangle,\widehat{g_{21}}(\rho_{NS})=\langle q_2,C(q_1,q_1,\bar{q_1})\rangle \quad (24)$$

The direction of NS bifurcation is determined by the sign of the first Lyapunov coefficient $l_2(\rho_{NS})$, which is defined as

$$l_2(\rho_{NS})=Re\left(\frac{\lambda_2\widehat{g_{21}}}{2}\right)-Re\left(\frac{(1-2\lambda_1)\lambda_2{}^2\widehat{g_{20}}\widehat{g_{11}}}{2(1-\lambda_1)}\right)-\frac{1}{2}|\widehat{g_{11}}|^2-\frac{1}{2}|\widehat{g_{02}}|^2 \quad (25)$$

In light of the aforementioned investigation, we present the following theorem regarding the direction and stability of the Neimark-Sacker bifurcation.

Theorem 2. *Suppose (19) is true and* $l_2(\rho_{NS})\neq 0$, *NS bifurcation will occur for system (9) at fixed point* $E(x^*,y^*)$ *if the* $\rho$ *changes its value in a tiny region around* $NS_E$. *Additionally, there exists an attractive (resp. repelling) smooth closed invariant curve bifurcate from* $E(x^*,y^*)$, *and the bifurcation is sub-critical(resp. super-critical) if* $l_2(\rho_{NS})<0$*(resp.* $l_2(\rho_{NS})>0$ ).

## 4. Numerical Simulations:

In this section, we will corroborate our theoretical findings for system (9) by numerical simulations. These numerical simulations will include bifurcation diagrams and phase portraits.

Example 1: The parameter values are chosen as follows $a=3.2,b=3.1,\rho=0.1092$ and , $\alpha$ varies in the range $0.35565\leq\ \alpha\leq 0.5988$. We find a fixed point $E(x^*,y^*)=(3.2,0.967)$ and for the system (9), the bifurcation point is $\alpha_F=0.5896$. The eigenvalues are $\lambda_{1,2}=-1,0.527794$. The associated eigenvectors are

$$q_1{\sim}(-0.76264,0.646824)^T \text{ and } q_2{\sim}(0.336167,0.941802)^T$$

For $<q_1,q_2>=1$, the normalized vector can then be taken as $\gamma_F=2.83442$.

From (17), we get $l_1(\alpha_F)=0.448314>0$. The Flip bifurcation is sub-critical as a result, and Theorem 1 is satisfied. Figure 1(a-b) shows that fixed point stability occurs for$\alpha>\alpha_F$, loses stability at $\alpha=\alpha_F$, and experiences a period doubling phenomena that results in chaos for $\alpha<\alpha_F$.We see the existence of the chaotic set and period -2 and -42 orbits for various values of $\alpha$. For various values of $\alpha\in[0.35565,0.5988]$, the phase picture of the bifurcations diagrams corresponding to Fig. 1 is shown in Fig. 2.

Example 2: The parameters that we choose for their values are $a=0.5,b=1.1,\rho=0.3466$ and $\alpha$ varies in the range $0.1\leq\alpha\leq 0.998$. At the fixed point $E(x^*,y^*)=(0.5,2.2)$, an NS bifurcation is visible and the critical value of the bifurcation point for the system (9) is $\alpha_{NS}=0.5896$. The eigenvalues are $\lambda,\bar{\lambda}=0.955002\pm 0.296591i$. These are the matching eigenvectors

$$q_1{\sim}(-0.143607-0.405663i,0.902671)^T \text{and } q_2{\sim}(0.902671,0.143607+0.405663i)^T$$

For $<q_1,q_2>=1$, then we can take the normalized factor $\gamma_{NS}=-1.03498\times 10^{-16}-1.36545i$.

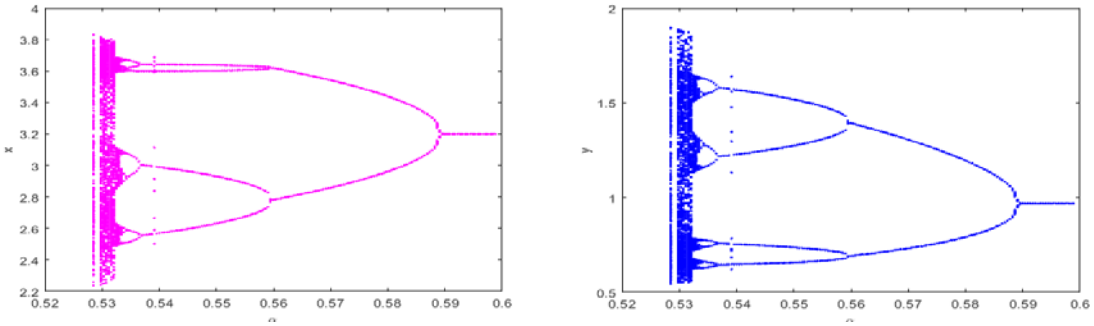


(a) (b)

**Figure 1. Flip Bifurcation diagram with $a=3.2,b=3.1,\rho=0.1092,\alpha\in[0.35565,\ 0.5988]$ $(x_0,y_0)=(3.2,0.967)$ in (a) $(\alpha,x)$ plane (b) $(\alpha,y)$ plane.**

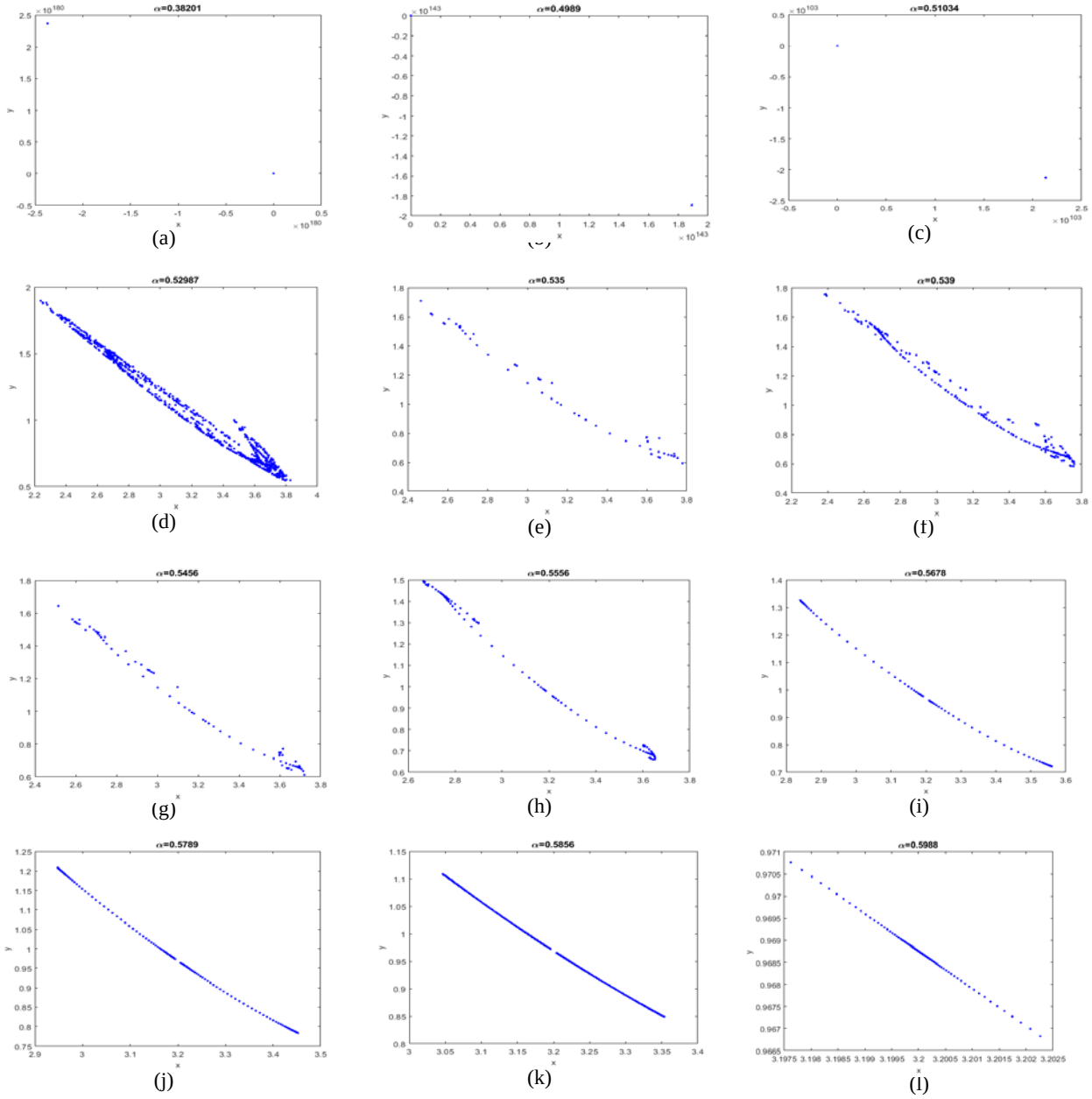


**Figure 2. Phase portraits for various values of αin accordance with Figure (1).**

Also,

$$\widehat{g_{20}} = 0.433261 - 0.482041i$$
$$\widehat{g_{11}} = -0.184628 + 0.345471i$$
$$\widehat{g_{02}} = 0.160011 - 0.628072i$$
$$\widehat{g_{21}} = -0.629245 - 1.17179i$$

From (25) we get $l_2(\rho_{NS}) = -1.05419 < 0$. As a result, the NS bifurcation is super-critical and Theorem 2 is satisfied.

The fixed point stability arises for $\alpha > \alpha_{NS}$, loses stability at $\alpha = \alpha_{NS}$, and an attracting invariant curve appears for $\alpha < \alpha_{NS}$, as can be seen from the bifurcation diagrams in Fig. 3(a-b). The smooth invariant curve's behavior is shown in detail in Fig. 4, phase portrait of bifurcation diagrams for various values of $\alpha \in [0.1, 0.998]$, which illustrates how it splits from the stable fixed point and expands in radius.

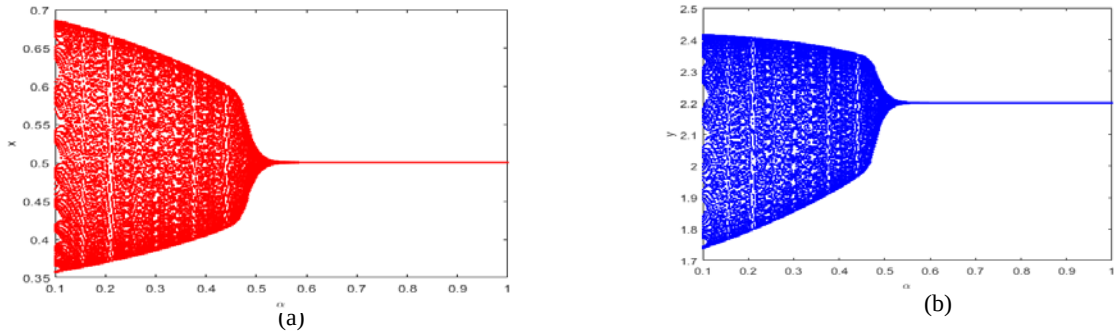

(a) (b)

**Figure 3. NS Bifurcation diagram with $a = 0.5, b = 1.1, \rho = 0.3466, \alpha \in [0.1, 0.998]$ $(x_0, y_0) = (0.5, 2.2)$ in (a) $(\alpha, x)$ plane (b) $(\alpha, y)$ plane.**

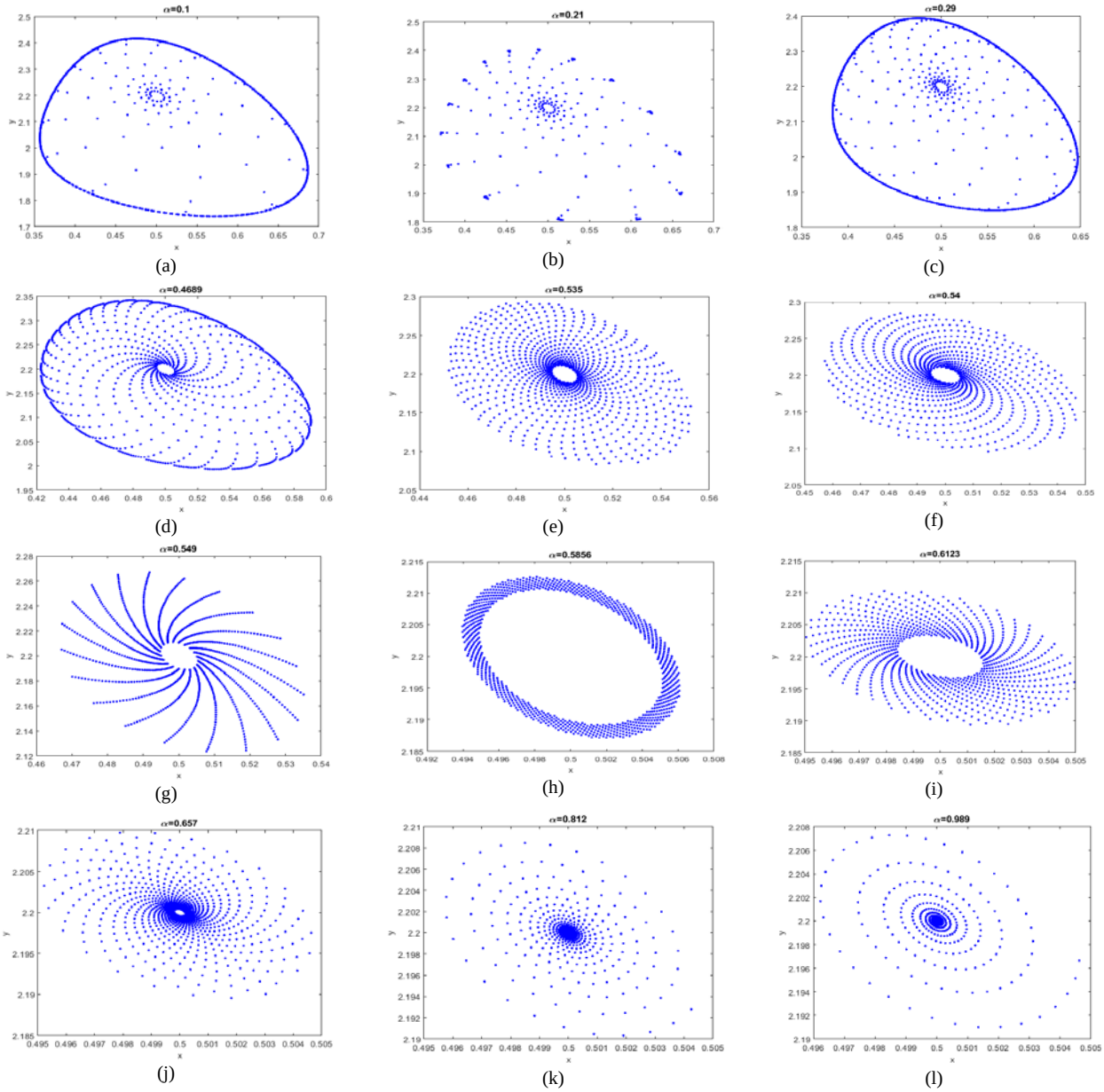


(a) (b) (c) (d) (e) (f) (g) (h) (i) (j) (k) (l)

**Figure 4. Phase portraits for various values of α in accordance with Figure (3).**

Example 3: As the values of $\rho$ change, the Brusselator system may exhibit more dynamic behavior in the Neimark-Sacker bifurcation diagram. A new Neimark-Sacker bifurcation diagram is created as shown in Fig. 5(a-b) when the parameter values are set as in Example 2 with $\alpha = 0.5896$ and $\rho$ ranging between $0.151565 \leq \rho \leq 1.99$. At $\rho = \rho_{NS} \sim 0.3889$, a Neimark-Sacker bifurcation occurs in the system. The phase portrait of the bifurcation diagrams for various values of $\rho$ in Fig. 6 provide a detailed illustration of the behavior of the smooth invariant curve.The smooth invariant curve is shown in this figure to split away from the steady fixed point and grow in radius.Additionally, periodic windows with attracting chaotic sets are discovered on the route to chaos.

## 5. Chaos Control

Chaos management is a difficult problem. We offer Hybrid control approach to control chaos in the fractional order Brusselator model. The classical hybrid control method developed by [29] controls period-doubling bifurcations and chaos in a discrete nonlinear dynamical system [30] by combining parameter perturbation with state feedback. In addition, the authors of [27] used a hybrid control method to prevent Neimark-Sacker bifurcation in a discrete-time prey-predator system. We offer Hybrid control approach to NS bifurcation in the fractional order Brusselator model.

For using hybrid control approach, we rebuild our uncontrolled system (9) as

$$X_{n+1} = G(X_n, \alpha, \rho) \tag{26}$$

where $X_n \in \mathbb{R}^2, G(.)$ is non-linear vector function and $\rho \in \mathbb{R}$ bifurcation parameter. The controlled system of (26), when hybrid control approach is used, becomes

$$X_{n+1} = \ddot{\omega} G(X_n, \alpha, \rho) + (1 - \ddot{\omega}) X_n \tag{27}$$

where $0 < \ddot{\omega} < 1$ is the control parameter.Now, if we apply the control approach indicated above to system (9), we obtain the controlled system shown below.

$$\begin{aligned} x_{n+1} &= \ddot{\omega}\left(x_n + \frac{\rho^\alpha}{\alpha\Gamma(\alpha)}(a - (1+b)x_n + {x_n}^2 y_n)\right) + (1 - \ddot{\omega})x_n \\ y_{n+1} &= \ddot{\omega}\left(y_n + \frac{\rho^\alpha}{\alpha\Gamma(\alpha)}(bx_n - {x_n}^2 y_n)\right) + (1 - \ddot{\omega})y_n \end{aligned} \tag{28}$$

For the controlled system (28), the Jacobian matrix at fixed point $E^+(x^+, y^+)$ (which is a fixed point of system (9)) takes the form

$$J(x^+, y^+) = \begin{pmatrix} (1 + (-1 + 2x^+y^+ - b)\ddot{\omega}\frac{\rho^\alpha}{\Gamma(1+\alpha)}) & {x^+}^2\ddot{\omega}\frac{\rho^\alpha}{\Gamma(1+\alpha)} \\ (-2x^+y^+ + b)\ddot{\omega}\frac{\rho^\alpha}{\Gamma(1+\alpha)} & 1 - {x^+}^2\ddot{\omega}\frac{\rho^\alpha}{\Gamma(1+\alpha)} \end{pmatrix}$$

Then the zeros of $|\ddot{\mu} - J(x^+, y^+)|$ (eigenvalues of J) satisfy the equation

$$\ddot{\mu}^2 + \ddot{\tau}_1\ddot{\mu} + \ddot{\tau}_0 = 0 \tag{29}$$

where

$$\begin{aligned} \ddot{\tau}_1 &= -2 + (1 + {x^+}^2 - 2x^+y^+ + b)\ddot{\omega}\left(\frac{\rho^\alpha}{\Gamma(1+\alpha)}\right) \\ \ddot{\tau}_0 &= 1 - (1 + {x^+}^2 - 2x^+y^+ + b)\ddot{\omega}\frac{\rho^\alpha}{\Gamma(1+\alpha)} + {x^+}^2\ddot{\omega}^2\left(\frac{\rho^\alpha}{\Gamma(1+\alpha)}\right)^2 \end{aligned}$$

Lemma 2: *If the uncontrolled systems fixed point $E^+(x^+, y^+)$ is unstable, then the controlled system (28) is a sink (stable) for it if the roots of (29) are inside an open disk and the criteria in Lemma 1 are met.*

Example 3: To assess the hybrid control methods effectiveness in minimizing chaotic (unstable) system dynamics, we fix $a = 0.5, b = 1.1, \alpha = 0.5896$ with $\rho = 0.25 < \rho_{NS}$. Then, it shows that the fixed point $E(0.5,2.21)$ of system (9) is unstable (see Fig 5 (a)-(b)), but this fixed point is stable for the controlled system (28) if $0 < \ddot{\omega} < 0.3756$. The fixed point $E$ is revealed to be a sink for the controlled system (28) in Figure 5(c) by taking $\ddot{\omega} = 0.3656$, which eliminates the unstable system dynamics around $E$. Additionally, we display the NS bifurcation diagrams of system (28) for several choices of $\ddot{\omega}$ and show that the system is under control when $\ddot{\omega} = 0.3656$.

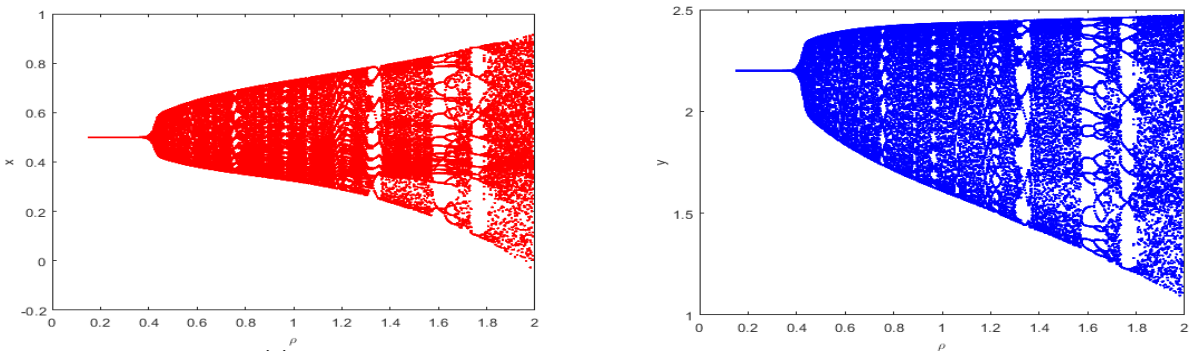


(a) (b)

**Figure 5. NS Bifurcation diagram with $a = 0.2, b = 0.9, \alpha = 0.5896, \rho \in [0.13, 0.37]$ $(x_0, y_0) = (0.9, 0.891)$ in (a) $(\rho, x)$ plane (b) $(\rho, y)$ plane.**

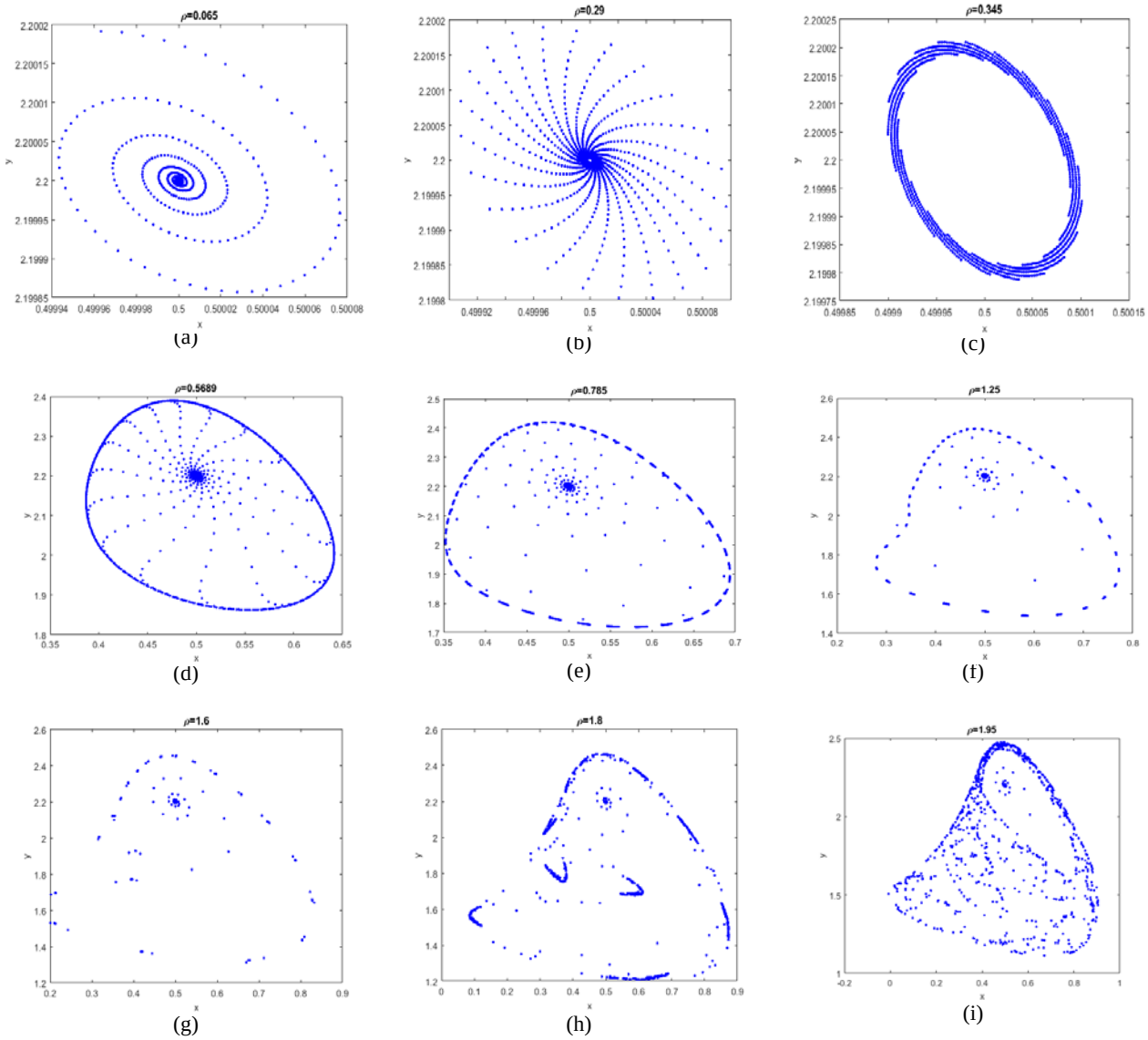


(a) (b) (c)

(d) (e) (f)

(g) (h) (i)

**Figure 6. Phase portrait for different values of ρ corresponding to Figure (5).**

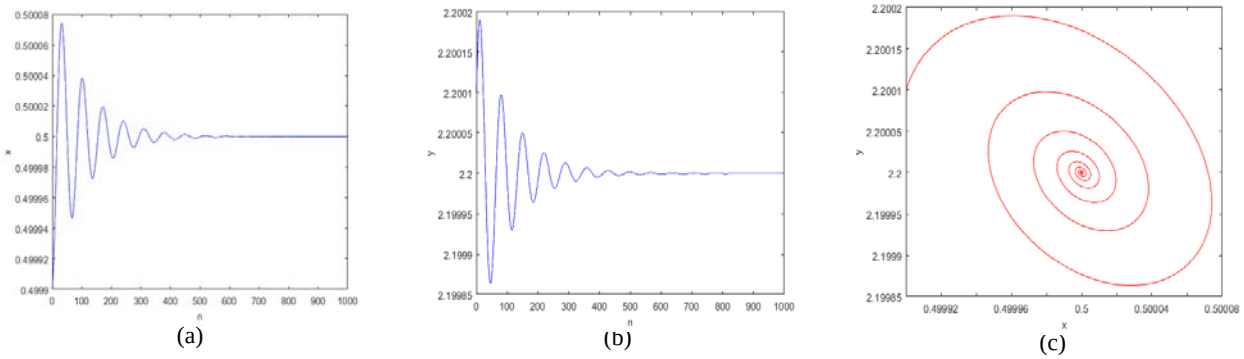


**Figure 7. Controlling the system's (28) chaos. (a) Time history of $x, y$ (b) Phase diagram of system (28).**

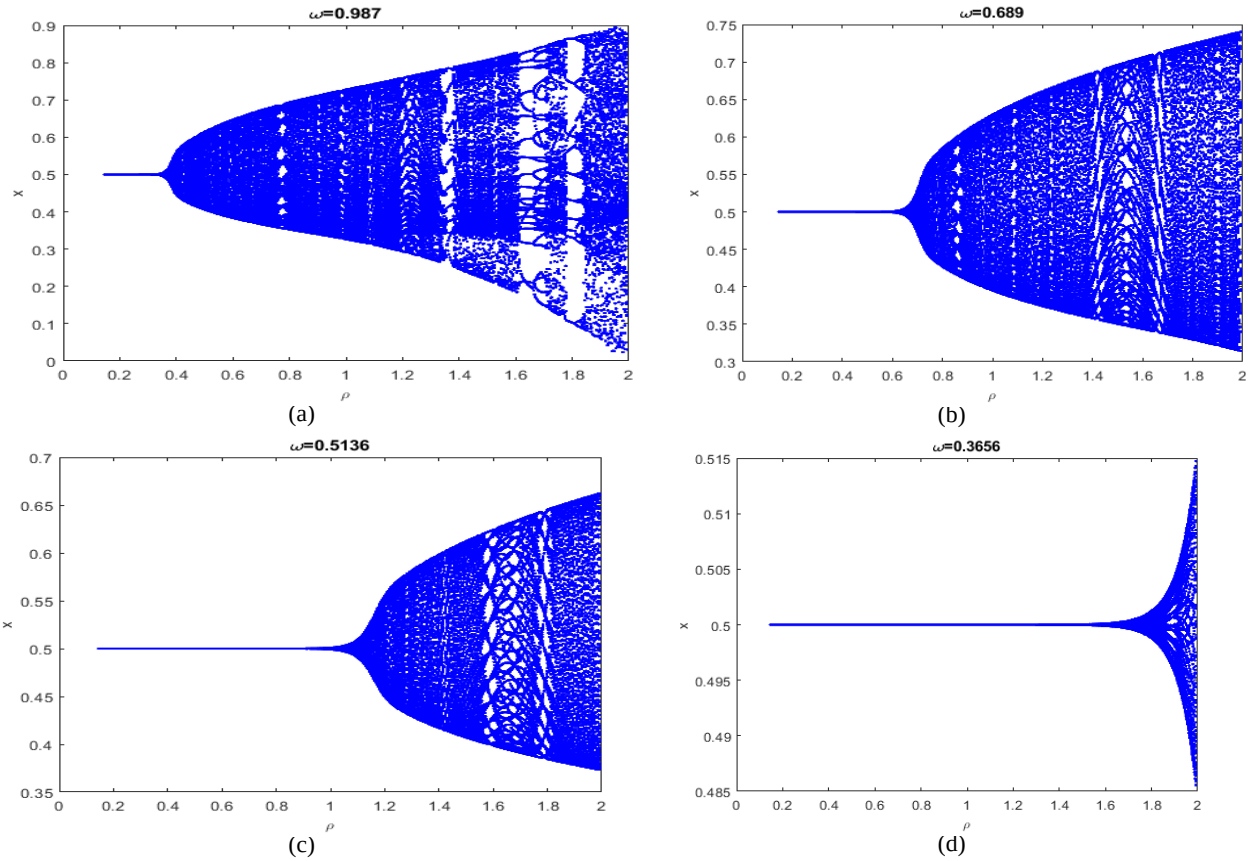


**Figure 8. NS bifurcation in $x$ for $(a)\ddot{\omega} = 0.987, (b)\ddot{\omega} = 0.689, (c)\ddot{\omega} = 0.5136, (d)\ddot{\omega} = 0.3656$.**

## 6. Conclusion

A new fractional order Brusselator model is discussed in this work. Such a fractional order model is derived from the Caputo fractional derivative concept. We show that if $\alpha$ fluctuates around the sets $PD_E$ or $NS_E$, the system (9) can experience a bifurcation (flip or NS) at a specific positive fixed point $E$ by applying the center manifold theorem and bifurcation theory.

As the parameters $\alpha$and$\rho$ are altered, the model exhibits a variety of intricate dynamical behaviors, including the emergence of flip and NS bifurcations, period-2, and 42 orbits, quasi-periodic orbits, attracting invariant circles, and chaotic sets.

Furthermore, we can see that stabilizing the dynamical system$(9)$ by choosing the appropriate value of. The two bi-

furcations cause the system to quickly go from steady state to chaotic dynamical behavior by opening up paths from periodic and quasi-periodic states; alternatively, chaotic dynamics appear or disappear simultaneously with the emergence of bifurcations. Last but not least, we use a hybrid control strategy to eliminate unstable system trajectories. Though the topic of investigating many parameter bifurcation in the system is still challenging. Additional analytical discoveries on this subject are expected to come from future study.

## References


[1] Kuznetsov, Y.A., Piccardi, C. (1994). Bifurcation analysis of periodic SEIR and SIR epidemic models. J. Math. Biol. 32, 109-121.

[2] Hethcote, H.W., Driessche, P.V. (1995). An SIS epidemic model with variable population size and delay. J. Math. Biol. 34, 177-194.

[3] Richard Magin, Manuel D. Ortigueira, Igor Podlubny, Juan Trujillo. (2011). On the fractional signals and systems. 91(3), 350-371.

[4] Chengdai Huang, Jinde Cao, Min Xiao, Ahmed Alsaedi, Fuad E. Alsaadi. (2017). Controlling bifurcation in a delayed fractional predator–prey system with incommensurate orders. Applied Mathematics and Computation, 293, 293-310.

[5] Chengdai Huang, Jinde Cao, Min Xiao, Ahmed Alsaedi, Tasawar Hayat. (2017). Bifurcations in a delayed fractional complex-valued neural network. Applied Mathematics and Computation, 292, 210-227.

[6] Chengdai Huang, Jinde Cao, Min Xiao, Ahmed Alsaedi, Tasawar Hayat. (2018). Effects of time delays on stability and Hopf bifurcation in a fractional ring-structured network with arbitrary neurons. Communications in Nonlinear Science and Numerical Simulation, 57, 1-13.

[7] Chengdai Huang, Yijie Meng, Jinde Cao, Ahmed Alsaedi, Fuad E. Alsaadi. (2017). New bifurcation results for fractional BAM neural network with leakage delay. Chaos, Solitons & Fractals, 100, 31-44.

[8] Al-Khaled, K., Alquran, M. (2014). An approximate solution for a fractional model of generalized Harry Dym equation. J. Math. Sci. 8, 125-130.

[9] Bagley, R. L. and Calico, R. (1991). Fractional order state equations for the control of visco elastically damped structures. Journal of Guidance, Control, and Dynamics, 14(2), 304-311.

[10] Ichise, M., Nagayanagi, Y., Kojima, T. (1971). An analog simulation of non-integer order transfer functions for analysis of electrode process. J. Electroanal. Chem. Interfacial Electrochem. 33, 253-265.

[11] Ahmad, W.M., Sprott, J.C. (2003). Chaos in fractional-order autonomous nonlinear systems. Chaos Solitons Fractals 16, 339-351.

[12] Podlubny, I. (1999). Fractional Differential Equations. New York: Academic Press.

[13] Hossein Jafari, Varsha Daftardar-Gejji. (2006). Solving a system of nonlinear fractional differential equations using Adomian decomposition. Journal of Computational and Applied Mathematics, 196(2), 644-651.

[14] I. Ameen, P. Novati. (2017). The solution of fractional order epidemic model by implicit Adams methods. Applied Mathematical Modelling, 43, 78-84.

[15] Shaher Momani, Zaid Odibat. (2007). Numerical approach to differential equations of fractional order. Journal of Computational and Applied Mathematics, 96-110.

[16] Elsadany, A. A., Matouk, A. E. (2015). Dynamical behaviors of fractional-order Lotka–Volterra predator–prey model and its discretization. Journal of Applied Mathematics and Computing, 49, 269-283.

[17] Ercan Balci, Senol Kartal, Ilhan Ozturk. (2021). Comparison of dynamical behavior between fractional order delayed and discrete conformable fractional order tumor-immune system. Math. Model. Nat. Phenom, 16(3).

[18] Ercan Balcı, İlhan Öztürk, Senol Kartal. (2019). Dynamical behaviour of fractional order tumor model with Caputo and conformable fractional derivative. Chaos, Solitons & Fractals, 123, 43-51.

[19] Abdelaziz, M.A.M., Ismail, A.I., Abdullah, F.A. et al. (2018). Bifurcations and chaos in a discrete SI epidemic model with fractional order. Adv Differ Equ, 2018(44).

[20] Khan, Abdul Qadeer & Khalique, Tanzeela. (2020). Neimark-Sacker bifurcation and hybrid control in a discrete-time Lotka-Volterra model. Mathematical Methods in the Applied Sciences, 43(9), 5887-5904.

[21] Khan, AQ, Bukhari, SAH & Almatrafi, MB. (2022). Global dynamics, Neimark-Sacker bifurcation and hybrid control in a Leslie's prey-predator model Global dynamics, Neimark-Sacker bifurcation and hybrid control in a Leslie's prey-predator model. Alexandria Engineering Journal, 61(12), 11391-11404.

[22] I. Prigogine, R. Lefever. (1968) Symmetry breaking instabilities in dissipative systems. II. J. Chem. Phys. 48, 1695-1700.

[23] G. Nicolis, I. Prigogine. (1977). Self-Organizations in Non-equilibrium Systems (Wiley-Interscience, New York).

[24] Kuznetsov, Y. (1998). Elements of applied bifurcation theory (Vol. 112). New York, USA: Springer Science and Business Media.

[25] Wen, G. (2005). Criterion to identify hopf bifurcations in maps of arbitrary dimension. Physical Review E, 72(2), 026201.

[26] Yao, S. (2012). New Bifurcation Critical Criterion of Flip-Neimark-Sacker Bifurcations for Two-Parameterized Family of n -Dimensional Discrete Systems. Discrete Dynamics in Nature and Society, 2012, 264526.

[27] Yuan, L. G., Yang, Q. G. (2015). Bifurcation, invariant curve and hybrid control in a discrete-time predator-prey system. Applied Mathematical Modelling, 39(8), 2345-2362.

[28] S.H. Strogatz. (1994). Nonlinear Dynamics and Chaos with Applications to Physics, Biology, Chemistry, and Engineering (Addison-Wesley, New York).

[29] X.S. Luo, G.R. Chen. (2003). B.H.Wang, Hybrid control of period-doubling bifurcation and chaos in discrete nonlinear dynamical systems. Chaos Soliton Fractals 18, 775-783.

[30] J.L. Ren, L.P. Yu. (2016). Codimension-two bifurcation, chaos and control in a discrete-time information diffusion model. J. NonlinearSci. 26, 1895-1931.